# PERFORMANCE CHARACTERISTICS OF ELECTROCHEMICALLY IMPREGNATED NICKEL OXIDE ELECTRODES FOR ALKALINE BATTERIES

K. I. VASU, V. S. MURALIDHARAN*, M. RAMAKRISHNAN, G. PARUTHIMAL KALAIGNAN and N. JAYALAKSHMI

*Central Electrochemical Research Institute, Karaikudi-6 (India)*

## Summary

Nickel oxide electrodes are widely used as cathodes in alkaline batteries. The introduction of electroactive material can take place by chemical and electrochemical methods. The effects of various additives to nickel nitrate solutions, used to impregnate sintered nickel electrodes electrochemically, have been studied at different current densities. The variation in active material composition was determined using atomic absorption and infrared spectroscopy. Ideal conditions for the preparation of nickel oxide electrodes have been identified.

## Introduction

The impregnation of electroactive material may be carried out either by chemical [1, 2], thermal [3, 4], or by electrochemical methods [5 - 12]. Nickel hydroxide, or mixed hydroxides of nickel with zinc, cobalt, cadmium, and manganese, may be used as the electrode-active material. The present investigation deals with the electrolyte composition and cell operating conditions. The performance of the optimised electrode was investigated using atomic absorption and infrared spectroscopic methods.

## Experimental

### Preparation of nickel electrodes

Loose sintered nickel electrodes were prepared by depositing reduced Inco nickel 250 powder onto perforated, mild steel sheet current collectors. They were then sintered at 1173 K under a hydrogen atmosphere for 1 h. The porosity of the $7 \times 5.5 \times 0.2$ cm electrodes was found to be 70 - 80%.

---

*Author to whom correspondence should be addressed.

TABLE 1

Impregnating solutions

| Electrode | Electrolyte composition | pH |
|---|---|---|
| A | 3 M $Ni(NO_3)_2$<br>+0.25 M $Co(NO_3)_2$<br>+0.1 M $Cd(NO_3)_2$<br>+0.1 M $MnSO_4$<br>+0.1 M $ZnSO_4$ | 2 - 3 |
| B | A + 0.25 M $NaNO_2$ | 4 - 5 |
| C | B + HCOOH | 3 - 4 |
| D | A + Sodium acetate | 4 - 5 |
| E | A + HCOOH | 1 - 2 |
| F | B + $HNO_3$ | 1 - 2 |

Cells were constructed using the sintered nickel plaques as cathodes with high-purity nickel (99.5%) sheet anodes.

Impregnation was carried out at different cathodic current densities for 90 min in various electrolytes (Table 1) with the cathodes between two anodes.

## Preparation of activated iron electrodes

Loose sintered iron electrodes were prepared using steel sheets, onto which nickel had been deposited, as current collectors. A reduced electrolytic iron powder and iron oxide (Fe + 15% w/w α-$Fe_3O_4$ + 3% w/w Cu + 10% w/w CdO + 0.03% w/w FeS) mixture was spread uniformly onto the current collector and sintered at 1173 K for 1 h under a hydrogen atmosphere. The dimensions of the electrodes were 7 × 5.5 × 0.2 cm. They were cathodically treated in 6 M KOH solutions, containing 32 g $l^{-1}$ of elemental sulphur, at 303 K for 36 h at 8 mA $cm^{-2}$ using stainless steel anodes [13].

## Charge and discharge studies

Nickel–iron cells were assembled in a perspex container using two iron electrodes of higher capacity as counter electrodes in 6 M KOH + 0.63 M LiOH and a nylon cloth separator. Charging was at the $C/13$ rate for 20 h. The nickel electrodes were discharged to 150 mV with regard to Hg/HgO at the $C/4$, $C/5$, and $C/10$ rates.

## Analysis of the impregnated active material

An infrared spectrometer was used to obtain the vibrational spectrum, whilst an atomic absorption spectrometer was used to determine the composition of the active material in the acid media.

## Results

### Electrochemical impregnation

This method involves the cathodic precipitation of metallic hydroxides from nickel salt solutions. The compositions of the electrode active materials are given in Table 2. To maintain a pH of 1 - 2, either nitric acid or formic acid was introduced periodically during electrolysis. The highest zinc content was obtained in the electrode prepared from sodium acetate solution. The influence current density had on the performance of electrodes prepared from formic acid solution was demonstrated. Increasing the current density from 5.2 to 6.5 mA cm$^{-2}$ decreased the cadmium content from 9.9 to 5.6% and the manganese content from 3.5 to 2%, whilst the cobalt and zinc contents increased from 10.6 to 12.1% and 5.4 to 8.2%, respectively.

TABLE 2

Atomic absorption spectroscopic determination of the active material composition

| Electrode | Current density (mA cm$^{-2}$) | Composition of active material (%) | | | | |
|---|---|---|---|---|---|---|
| | | Ni | Mn | Cd | Co | Zn |
| A | 5.2 | 72.6 | 3.1 | 7.8 | 9.6 | 6.6 |
| B | 5.2 | 69.7 | 3.6 | 8.4 | 11.2 | 6.9 |
| C | 5.2 | 70.6 | 3.5 | 7.9 | 11.3 | 6.4 |
| D | 5.2 | 68.8 | 1.6 | 5.1 | 8.9 | 15.3 |
| E | 5.2 | 70.4 | 3.5 | 9.9 | 10.6 | 5.4 |
| E$_1$ | 4 | 71.7 | 2.3 | 6.3 | 11.4 | 8.1 |
| E$_2$ | 6.5 | 71.8 | 2.0 | 5.6 | 12.1 | 8.2 |
| F | 5.2 | 67.1 | 2.8 | 6.0 | 9.7 | 13.8 |

### Electrochemical studies

Figures 1 - 6 present the variation of nickel electrode potential with capacity at different discharge rates. An initial fall from between 400 and
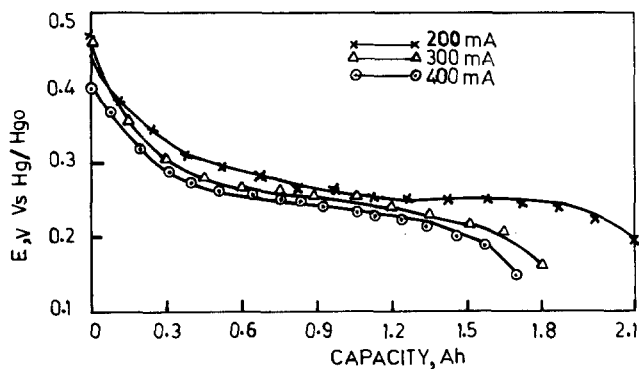


Fig. 1. Variation of nickel electrode (A) potential with capacity.
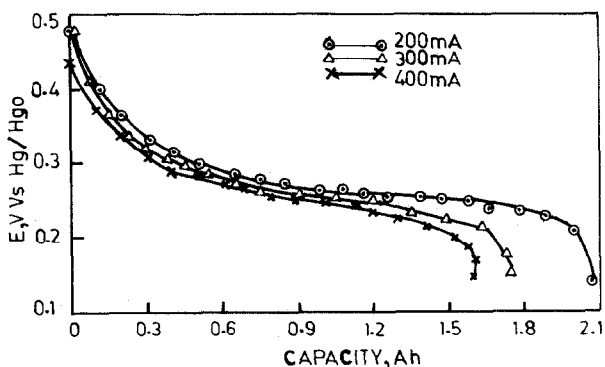
Fig. 2. Variation of nickel electrode (B) potential with capacity.
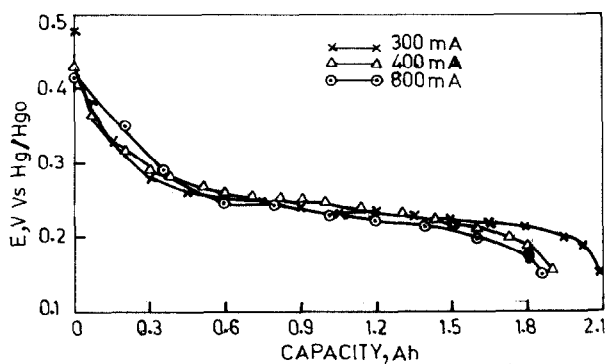


Fig. 3. Variation of nickel electrode (C) potential with capacity.

500 mV to less than 300 mV, followed by a more stable region was observed in all cases. Below 250 mV limiting current regions were observed.

## Discussion

An ideal reversible battery involving only mutually insoluble solid electrode phases requires that the slope of open circuit discharge ($V$ versus $Q$) be zero in the absence of activation overpotential, diffusion overpotential, internal resistance, and other complications arising from design [14]. Since the discharge curves were almost linear in the centre of the plateau, $dE/dQ$ at the 50% state of discharge was used to compare the reversible behaviour of the electrodes.

On a charged electrode, there will be capacity losses on standing, and the initial fall from +500 to +300 mV is due to the activation overpotential losses. In this potential range, oxygen evolution may accompany the reduction of higher valent oxides of nickel. A near-linear region from 300 to 250 mV is mostly due to the internal resistance and the polarisation resistance
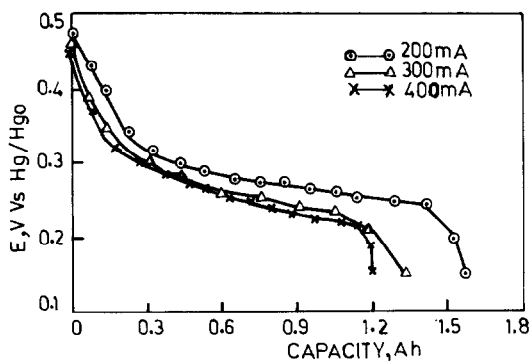
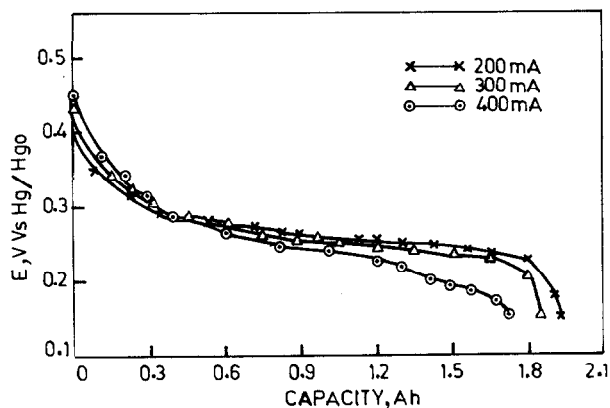Fig. 4. Variation of nickel electrode (D) potential with capacity.



Fig. 5. Variation of nickel electrode (E) potential with capacity.
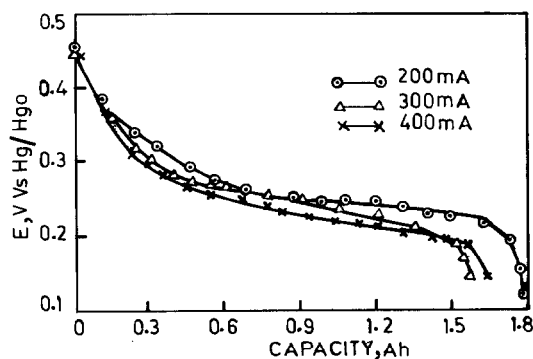


Fig. 6. Variation of nickel electrode (F) potential with capacity.

components of the electrode reaction. Below 250 mV, the appearance of a limiting current is due to the diffusion of hydroxyl ions inside the electrode pores. Between 300 and 250 mV, the reduction of higher-valent oxides of nickel to $Ni_3O_2(OH)_4$ is favoured [15].

TABLE 3

Parameters derived from discharge curves at different currents for impregnated nickel electrodes

| Electrode | $(dE^+/dQ)$ $Q = Q_0^+/2$ $(V/C) \times 10^{-3}$ | | |
| | 200 mA | 300 mA | 400 mA |
| --- | --- | --- | --- |
| A | 25.0 | 41.6 | 50.0 |
| B | 33.0 | 33.0 | 62.5 |
| C | — | 50.0 | 50.0 |
| D | 41.6 | 75.0 | 116.0 |
| E | 41.6 | 50.0 | 50.0 |
| F | 54.3 | 83.3 | 83.3 |

In this potential region, the discharge curves were analysed for $(dE/dQ)$ at 50% state of discharge. Table 3 shows that the minimum slope was obtained for electrode A at 200 mA discharge and the maximum for electrode D at 400 mA discharge. In the case of electrodes C and E the slope was almost independent of the discharge current. The highest slopes with electrode F were observed at 300 and 400 mA.

The performance characteristics of different nickel electrodes discharged at 400 mA are given in Table 4. The percentage of the total capacity utilised between 350 and 300 mV is compared in an attempt to determine the composition which gives best performance at near constant potential. Electrode E (17 - 93% utilisation) was the best, followed by D, A, C and F. The percentage utilisation was calculated from:

$$\text{Utilisation} = \frac{\text{Measured capacity}}{\text{Theoretical capacity}}$$

At 350 to 300 mV, it was observed that on a previously charged $Ni(OH)_2$ electrode· $\gamma$-phase (0.833 $NiO_2$, 0.167 $Ni(OH)_2$) (0.35 $H_2O$) (0.33

TABLE 4

Performance characteristics of impregnated nickel electrodes*

| Electrode | Theoretical capacity (mA h cm$^{-2}$) | Proportion of the total capacity falling within the 350 - 300 mV range (%) | Total capacity (mA h cm$^{-2}$) | Utilisation (%) |
| --- | --- | --- | --- | --- |
| A | 24.24 | 68 | 20.38 | 84 |
| B | 27.74 | 50 | 20.78 | 75 |
| C | 29.20 | 57 | 24.23 | 83 |
| D | 23.95 | 70 | 17.27 | 72 |
| E | 24.24 | 76 | 22.50 | 93 |
| F | 25.69 | 55 | 20.78 | 81 |

*Discharged at 400 mA.

KOH) was formed and reduced to an oxidation state of 2.7 [16 - 20]. The protonation of the $\gamma$-phase leads to

$$(NiOOH \cdot OH^- \cdot M^+ \cdot xH_2O) + H^+ + e \longrightarrow Ni_3O_2(OH)_4 + M^+ + yH_2O$$
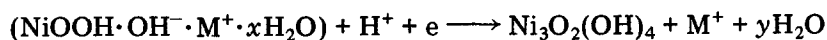
Voltammetric studies [21, 22] on zinc, cobalt, cadmium, and manganese co-precipitated with nickel hydroxide electrodes revealed that increasing the zinc content favoured nickel hydroxide oxidation and hindered the conversion of high valent oxides of nickel to lower valent oxides. Trivalent cobalt undergoes reductive dissolution to dicobaltite ion. Cadmium and manganese hydroxides favour the reversibility of the process. The poor utilisation of D is due to the high zinc and low cobalt contents, whereas the high utilisation of E is due to the increased cadmium content and low zinc content.

Figure 7 is the infrared spectrum of the electroactive material from electrode E which indicates the presence of hydrogen bonding. The dip in transmission at a wave number of 3440 cm$^{-1}$ is due to the stretching of the water molecules. The bending of these water molecules may occur, as evidenced by the trough at 1640 cm$^{-1}$. The sharp dip at 1380 cm$^{-1}$ suggests the presence of lattice-trapped or intercalated water molecules [23]. The remaining troughs on the spectra at 525, 450, and 340 cm$^{-1}$ are due to the bending, stretching of hydroxyl groups as a whole, relative to the nickel atom.
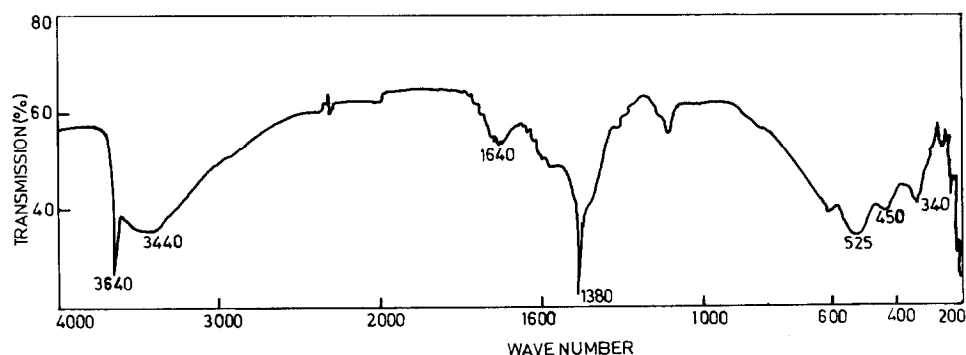


Fig. 7. IR spectra of the electroactive material from electrode E.

Studies on the platinum surface under potentiodynamic conditions revealed [24] that the inner layer of nickel hydroxide films was found to contain less water than the bulk of the film. The concentration gradient of the water molecules is responsible for the electrochemical activity of nickel oxide electrodes [15].

Conclusions

Studies on the effects of various additives to nickel oxide electrodes revealed that a composition prepared using a formic acid electrolyte at 5.2

mA cm$^{-2}$ so as to yield more cadmium and manganese, but less zinc, gave maximum percentage utilisation during discharge. The IR spectrum of this electrode material revealed the presence of intercalated water molecules.

# References

1 A. Fleischer, *Trans. Electrochem. Soc., 94* (1948) 289.
2 M. Paszkiewick, *J. Appl. Electrochem., 11* (1981) 135.
3 P. L. Bourgault, P. E. Lake and E. J. Casey, *Can. J. Technol., 34* (1957) 495.
4 Marian Wales, *Electrochim. Acta, 24* (1979) 629.
5 L. Kandler, *U.S. Pat. 3,214,355* (1965).
6 T. R. Williamson, *Ext. Abstr., The Electrochemical Society 158th Fall Meeting, Hollywood, FL, U.S.A., Oct. 5 - 10, 1980,* Vol. 80-2, p. 288.
7 E. Haeussler, in D. H. Collins (ed.), *Power Sources 1,* Pergamon Press, Oxford, 1967, p. 287.
8 E. J. McHenry, *Electrochem. Technol., 5* (1967) 275.
9 D. F. Pickett, Fabrication and investigation of nickel–alkaline cells, Part-I, *Tech. Rep., AFAPL-TR-75-34,* Oct. 1975.
10 E. J. McHenry and R. L. Beauchamp, *Ext. Abstr., The Electrochemical Society Fall Meeting, Cleveland, OH, U.S.A., Oct. 3 - 7, 1971,* Abstr. No. 6, p. 21.
11 Po-Yen Lu, *Proc. Symp. Advances in Battery Materials and Processes, 164th Meeting of the Electrochemical Society, Washington, DC, U.S.A., Oct 9 - 14, 1983,* Vol. 84-4, p. 218.
12 Kuo-Chuan Ho and Jacob Jorne, *AICHE, Symp. Series, 83* (1987) 87.
13 Robert J. McCormick, Yorktown Heights and Winslow. E. Ryan, *U.S. Pat. 3,525,640* (1970).
14 S. Satyanarayana, *Trans. SAEST, 11* (1976) 19.
15 V. S. Muralidharan, *B. Electrochem., 4* (7) (1988) 651.
16 R. Barnard and C. F. Randell, *J. Appl. Electrochem., 13* (1983) 27.
17 R. Barnard and C. F. Randell, *J. Appl. Electrochem., 13* (1983) 89.
18 R. Barnard and C. F. Randell, *J. Appl. Electrochem., 13* (1983) 97.
19 R. Barnard and C. F. Randell, *J. Power Sources, 9* (1983) 185.
20 M. Vissches and E. Barendrecht, *J. Electroanal. Chem., 154* (1983) 69.
21 G. Paruthimal Kalaignan, V. S. Muralidharan and K. I. Vasu, *10th Int. Congr. on Metallic Corrosion, Madras, India,* Vol. 1, Oxford & IBH Publishing Co, Pvt Ltd., India, 1987, p. 615.
22 G. Paruthimal Kalaignan, V. S. Muralidharan and K. I. Vasu, Electrochemical behaviour of impregnated nickel hydroxide electrodes, *Ind. J. Technol.,* in press.
23 Ravi Varma, *Prog. Batteries Solar Cells, 6* (1987) 22, J.E.C. Press Inc. (Japan).
24 R. E. Carbonio, V. A. Maoazno, A. C. Giordano, J. P. Vilche and A. J. Aravia, *J. Appl. Electrochem., 12* (1982) 121.